

Aspirin Restores Radiosensitivity in Cervical Cancer Cells by Inducing Mitotic Catastrophe through Downregulating G2/M Effectors

Salini Das¹, Dilip Kumar Ray², Debomita Sengupta¹, Elizabeth Mahapatra¹, Souvick Biswas¹, Madhumita Roy¹, Sutapa Mukherjee^{1*}

Abstract

Background/Aim: Compromised cell-cycle checkpoint is a major obstacle for rendering radiotherapeutic success of radioresistant cells. Aspirin (ASA), an anti-inflammatory agent was repurposed previously for improving radiotherapy by limiting radiation toxicity. However, the underlying mechanism was unclear. The present study aimed to identify the mechanism of ASA mediated reversal of radioresistance in cervical cancer cells. **Methods:** Radioresistant subline SiHa/RR was developed from parental cervical squamous carcinoma cell line SiHa by chronic fractionated irradiation (IR). The radioresistance property of SiHa/RR was confirmed by clonogenic assay. Alteration in cell-cycle by ASA was determined by flow cytometry. ASA induced nuclear damage as consequence of mitotic catastrophe was confirmed by microscopic observation. The interaction between ASA and G2/M regulators was explored through *in silico* docking analysis and expressional change of them was affirmed by western blotting. Immunofluorescence study to examine Aurora Kinase A localization in presence and absence of ASA treatment was conducted. Finally the radiosensitizing ability of ASA was verified by apoptotic parameters (flow cytometrically and by western blotting). **Result:** Higher colony forming ability of SiHa/RR compared to SiHa became restrained upon ASA (5 μ M) treatment prior to IR. Flow cytometric analysis of ASA treated cells showed increased G2/M population followed by enlargement of cells displaying giant multinucleated morphology; typical characteristics of mitotic catastrophe. Underlying noteworthy mechanisms involved decreased expressions of G2/M regulatory proteins (Cyclin B1, CDK1, Aurora A Kinase, pAurora A Kinase) in IR/ASA along with inhibiting nuclear localization of Aurora Kinase A in SiHa/RR. Docking results also supported the findings. Prolonged treatment (12 h) with ASA led to apoptosis by altering expressions of Bcl2, Bax and Cytochrome C; which was achieved through the event of mitotic catastrophe. **Conclusion:** This work established that G2/M arrest and mitotic catastrophe can be considered as the principle mechanism of restoration of radiosensitivity in SiHa/RR by ASA pretreatment.

Keywords: AURKA- ASA- Radioresistance- Mitotic Catastrophe

Asian Pac J Cancer Prev, 23 (11), 3801-3813

Introduction

Cervical cancer being the fourth common cancer in women is posing a major threat due to its increasing events of recurrence (Sung et al., 2021). Radiotherapy, the primary treatment modality of cervical cancer, executes its action by instigating DNA damage, cell-cycle arrest and oxidative stress (Bader et al., 2021; Mavragani et al., 2019; Marill et al., 2019). However, development of acquired radioresistance is the principal hindrance behind the reduced efficacy of radiotherapy (Galeaz et al., 2021; Schulz et al., 2019). Acquired radioresistance is manifested at the molecular level by sequestering adaptive alterations within the cells, tissues and finally

to tumor. These transformations include development and persistence of efficient repair system, degradation of DNA damage sensors subsequently leading to cell-cycle progression and proliferation (Domogaur et al., 2021; Huang et al., 2020; Alsubhi et al., 2016; Lim et al., 2012; Zhao et al., 2012). Mitotic progression being one of the prevalent radioresistant properties raises attention of the researchers. Mitotic serine threonine kinases which are the effective regulators of sequential mitotic events, act as prospective players to achieve such alterations in cells (Hauge et al., 2021). Aurora Kinase A is such a well characterized mitotic serine threonine kinase, predominantly accountable for G2/M progression of cell-cycle (Shen et al., 2019; Liu et al., 2019; Woo et al.,

¹Department of Environmental Carcinogenesis & Toxicology, Chittaranjan National Cancer Institute, Kolkata, India. ²Department of Medical Physics, Chittaranjan National Cancer Institute, Kolkata, India. *For Correspondence: sutapa_c_in@yahoo.com

2015; Mandati et al., 2019) by promoting mitotic exit, stabilization of centrosome, and regulation of proper spindle dynamics (Luisa Barretta et al., 2016). Regardless of its activity, overexpression of Aurora Kinase A triggers adaptive mechanisms rendering radioresistance in cancer cells against radiation induced mitotic arrest or mitotic slippage (Marxer et al., 2014). Therefore attempting to revamp cytotoxicity is highly entailed for the reversal of resistance. Radiosensitizers in this context can be considered as promising molecules which makes the target cells susceptible towards radiation (Gong et al., 2021). Cells exert variations in radiosensitivity at different phases of cell-cycle making G2/M phase the most radiosensitive of them (Otani et al., 2016). Accordingly, radiosensitizers tend to arrest the cell-cycle at G2/M phase by activating cell-cycle checkpoint regulators (Morgan et al., 2015; Huang et al., 2020; Qian et al., 2022, El-Benhawy et al., 2021). But in case of radioresistant cells, these checkpoint regulators are either inactive or too deregulated thereby escape arrest and subsequent cell death (Visconti et al., 2016). Therefore, inducing mechanisms of cell killing in compromised checkpoint conditions should be thoroughly investigated. Mitotic catastrophe is a phenomenon of proliferation arrest occurring as a result of DNA damage or inappropriate spindle arrangement in checkpoint deficient condition. This event is characterized by formation of giant cells with multiple nucleus and/or micronucleus (Sazonova et al., 2021). Therefore, attempts to utilize this specialized cell death mechanism to restore radiosensitivity in radioresistant cells can be accounted as novel therapeutic strategy. Perceiving the urgency of this issue, induction of mitotic catastrophe by repurposing conventional drugs is a wiser option than developing novel radiopharmaceuticals. Aspirin (ASA), a well known NSAID (Non-Steroidal Anti Inflammatory Drug) with multiple therapeutic applications is nowadays getting attention in cancer research due to its antiproliferative property (Bagheri et al., 2018). Reports suggest that the inhibitory effect of ASA on COX1/2 prevents the cancer induced inflammation and cell proliferation (Jiang et al., 2020). Based on these previous findings, the aim of the present study was to enquire the radiosensitizing potential of ASA with special emphasis on occurrence of mitotic catastrophe and its underlying mechanism in this context.

Materials and Methods

Chemical reagents

The primary antibodies used for the study, anti-FITC-conjugated anti-rabbit IgG were purchased from Genetex, CA, USA. Antibodies against Aurora Kinase A and pAurora Kinase A(T288) were purchased from Cell Signaling Technology, MA, USA. CDK1, Cyclin B1, Bax, Bcl2, Cytochrome C was procured from Biologend, CA, USA. β actin, PCNA, Ki-67 antibodies were procured from Santa Cruz, Texas, USA. Fetal Bovine Serum was purchased from Gibco (Thermo Fisher Scientific), MA, USA. Aspirin, BSA (Bovine Serum Albumin), PI (Propidium Iodide), DAPI (4',6-diamidino-2-phenylindole), Crystal Violet were purchased from Sigma-Aldrich, USA. Giemsa stain was purchased from Merck,

Germany. Annexin V FITC assay kit was purchased from Cayman Chemical, Michigan, USA. All other reagents of analytical grade were procured locally.

Cell lines and cell culture

Human cervical squamous carcinoma cell line SiHa was purchased from National Centre for Cell Science (NCCS), Pune, INDIA. Subsequently, a radioresistant subline SiHa/RR was developed from SiHa by weekly incremental fractionated irradiation doses and finally a colony was isolated at 40 Gy; designated as SiHa/RR. Both SiHa and SiHa/RR cells were maintained in MEM supplemented with 15% heat inactivated fetal bovine serum (FBS) and antibiotics (gentamycin 40 μ g, penicillin 100 units, streptomycin 10 μ g/ml). Cells were maintained at 37°C in a humidified CO₂ incubator having 5% CO₂/95% air.

Irradiation Protocol

SiHa cells were initially cultured to reach an approximate confluence of 50% in 25 cm² cell culture flasks (Greiner Bio-One International). The culture medium was replenished with 2 ml of fresh complete MEM 15 min prior to exposure to radiation dose. Flasks were irradiated using X-Ray linear accelerator (Elekta). Medium of the post-irradiated cultured flask was replaced with 5 ml fresh medium before further incubation. Surviving cells were allowed to repopulate until reaching maximum confluency and then again subcultured into two new flasks after proper trypsinization. Upon attaining 50% confluency, these cells were subjected to another round of irradiation in the following week. The initial doses of irradiation being 2 Gy, successive weekly incremental doses of 0.5 Gy were administered and finally radioresistant subline was isolated after 20 weeks with total cumulative doses of 40 Gy. A weekly maintenance dose of 2 Gy was continued to the cultured flask of isolated subline for sustaining adaptability of the cells. Further experiments were accomplished with exponentially growing cells after 48 h of the last maintenance irradiation dose.

Determination of optimum concentration of ASA by MTT assay

To estimate the optimum treatment concentration of ASA for the successive experiments, MTT (3-(4,5-Dimethylthiazol-2-yl)-2,5-Diphenyltetrazolium Bromide) assay was performed. Cells were seeded in 96 well plates (1x10⁴) and were treated with a wide range of concentrations of ASA (1-1000 μ M) for 24 h. Medium was discarded thereafter and the cells were treated with MTT solution 50 μ l (1.2 mg/ml in water) for 5 h. Plated cells were centrifuged at 1000 rpm for 5 min. The supernatant was discarded and volume was replenished using DMSO to dissolve MTT-formazan product. The optical density value of purple colored final products signifying viable cells was estimated in spectrophotometer (TECAN) at absorbance maxima of 570 nm.

Intracellular uptake of ASA

Intracellular uptake of ASA was determined using its auto-fluorescence property. SiHa and SiHa/RR cells

were seeded (1×10^5) and upon reaching confluency, cells were incubated with ASA ($5 \mu\text{M}$) for 6 h. Treated cells were trypsinized and cell lysates were prepared using NP 40 lysis buffer. Cell lysates were then treated with 4M NaOH for ionization to enhance the fluorescence. The fluorescence intensity was measured at the excitation wavelength 290 nm and emission wavelength 460 nm in spectrofluorimeter (Varian). Fluorescence intensity values were plotted graphically.

Treatment design

For successive experiments SiHa and SiHa/RR cells were batched into four groups (A). Untreated (UT), (B) Irradiated with 4 Gy (IR), (C) Treated with $5 \mu\text{M}$ ASA for 6 h (ASA), (D) Treated with $5 \mu\text{M}$ ASA for 6 h with 4 Gy irradiation (ASA+IR). Apoptosis study was conducted with ASA treatment duration for 12 h with IR (8Gy).

Clonogenic viability assay

Confirmation of acquired radioresistance was evaluated by colony formation assay. Cells at a number of 1,000 per well were seeded in 6-well plate and incubated for 24 h. In another set of experiments cells were pre-treated with ASA as mentioned in treatment design (D). Afterwards, both SiHa and SiHa/RR cells were irradiated with an acute dose of 2, 4, 6, 8 Gy. Cells were allowed to grow till visible colonies were found (~3 weeks). Colonies were washed with PBS, fixed in methanol: acetic acid fixative (3:1) and subsequently stained with 0.5% crystal violet dissolved in methanol. Colonies of 50 or more cells were counted under inverted microscope (Olympus). Surviving fraction (SF) was calculated using the formula- number of colonies formed after irradiation/total number of cells seeded x plating efficiency.

Microscopic observation of nuclear morphology

For examining the distinguishing morphological features, both SiHa and SiHa/RR cells were plated (1×10^5) in 6 well plate. Culture was maintained till attaining logarithmic growth phase and cells were treated according to the above mentioned doses. After completion of incubation period, cells were fixed with methanol: acetic acid fixative (3:1) for 15 mins. Cells were stained with Giemsa stain (5% solution prepared in Sorenson's phosphate Buffer pH 7.2, 0.133M Na_2HPO_4 , 0.133M KH_2PO_4) and examined under a Phase contrast microscope (Olympus).

In a second set of experimentation, both treated and untreated cells (1×10^5), seeded in coverslips were stained with DAPI ($1 \mu\text{g/ml}$) after fixing the cells with 2% paraformaldehyde solution in PBS for 10 min at room temperature followed by repeated washing with 1X PBS. Coverslips were mounted on poly L-Lysin coated slides using DPX and were observed under fluorescence microscope at DAPI specific filter (Leica).

Cell-cycle and cell size analysis by flow cytometry

Cell-cycle phase specific distribution of parental vs. radioresistant cells was evaluated using flow cytometry technique. Treated/untreated SiHa and SiHa/RR (2×10^6 cells) were suspended in cold PBS and centrifuged

at 400 g for 8 min. Successive fixation of cells were done in 70% cold absolute ethanol and were incubated in ice for 30 min. Cell pellets obtained after centrifugation and removal of ethanol were suspended in 1ml DNA binding solution ($200 \mu\text{g/ml}$ RNase + $50 \mu\text{g/ml}$ PI) and kept in dark for 30 min before analysis in BD LSR Fortessa Flow Cytometer. Fluorescence was captured on FL2H channel and 10,000 cells with logarithmic amplification were counted. Cell size was analysed by gating the cells in side scatter vs forward scatter axis.

Annexin V-FITC/PI staining for identifying apoptotic cells

To assess the degree of apoptosis in experimental cells treated with either ASA or IR or both, Cayman's Annexin V FITC assay kit was employed. Confluent cells achieved after requisite treatment were trypsinized and centrifuged at 400g for 5 min at 4°C . Cells were resuspended in 1X binding buffer for another course of centrifugation. Cells were stained with $50 \mu\text{l}$ Annexin V/PI staining solution and were incubated in dark for 10 min. Finally, $150 \mu\text{l}$ 1X binding buffer was added to ensure analysis of cells in BD LSR Fortessa flowcytometer using an excitation wavelength of 488 nm and an emission wavelength of 525 nm for FITC and 655-730 nm for PI.

Immunofluorescence

Cells (1×10^5) were seeded on a cover slip and placed in 6 well plates for 24 h before irradiation. Cover slips with post irradiated cells were incubated further for 6 h and then rinsed twice with PBS and fixed with 2% paraformaldehyde in PBS for 10 min at RT. Afterwards, cells were kept in permeabilization buffer containing 0.5% Triton X-100 in PBS (PBST) for 10 min at 4°C . Subsequent two more washings with PBST cells were incubated in blocking solution consisting of PBST with 2% BSA for 30 min. Cells were then coated with anti- Aurora Kinase A primary antibody and kept for 2 h at RT. Cover slips were washed five times with PBST (PBS+0.1% Tween 20) for 5 min each and fluorescein isothiocyanate (FITC)-conjugated secondary antibody was added and kept additionally at 37°C for 2 h. Counterstaining of the cells was done with DAPI and cells were mounted on microscopic slides by DPX. Immunostained Aurora Kinase A foci were observed using a fluorescence microscope (Leica TCS SP8 confocal microscope). Images were visualized and analyzed in Las X software.

Western Blotting

Protein expression was determined by immunoblotting technique followed in the laboratory (Biswas et al., 2021). Cell lysates were prepared using lysis buffer. Bradford colorimetric assay was undertaken for quantifying protein concentration. Electrophoresis of equal amounts of total proteins were performed on SDS-polyacrylamide gel using electrophoresis buffer (Tris: 25 mM, glycine: 192 mM, SDS: 20%) (Bio-Rad apparatus) and electro-transferred to nitrocellulose membranes using transfer buffer (Tris: 250 mM, glycine: 192 mM, methanol: 10%). Membranes were blocked in 5% BSA, incubated overnight with primary antibodies at 4°C and were washed with TBST (Tris Buffered Saline with Tween 20) thrice. Alkaline

phosphatase-conjugated anti-mouse IgG or anti-rabbit IgG(1:1,000 dilutions in TBS) was added to it. Washing with TBST was performed prior to addition of BCIP/NBT to visualize the proteins. The comparative expression profiles of Ki-67, PCNA, Aurora Kinase A, pAurora Kinase A(T288), Cyclin B1, CDK1, Cytochrome C, Bax, Bcl2 was assessed using β -actin as loading control.

In silico analysis

String Database was used to study the interactions between the overexpressed proteins in SiHa/RR cells based on the formula; Network analysis = Network Enrichment Analysis + Network Topological Analysis. *in silico* docking analysis of ASA and Cyclin B1; ASA and CDK1 and ASA and Aurora Kinase A was performed using FireDock software and was visualized using pymol software.

Statistical Calculation

Comparative analysis of differences between groups was carried out using Student's t test in the GraphPad Prism 5.0 software package (GraphPad Software, Inc., La Jolla, CA, USA). $p < 0.001$ was considered the minimal

level of significance. Data or values were obtained from at least three independent experiments and expressed as Mean \pm SD.

Results

Confirmation of acquired radioresistance in SiHa/RR

A radioresistant cervical squamous carcinoma cell line (SiHa/RR) was developed by subjecting parental SiHa cells to chronic irradiation with initial dose of 2 Gy followed by a weekly incremental dose of 0.5 Gy. Finally, the subline was isolated at a cumulative dose of 40 Gy. The developmental procedure has been schematically depicted (Figure 1A). Isolated radioresistant subline was maintained at a weekly radiation of 2 Gy. The radioresistant property of SiHa/RR was confirmed by performing clonogenic viability assay. Both SiHa and SiHa/RR cells were challenged with acute doses of 2, 4, 6, 8 Gy of radiation. Crystal violet stained colonies showed high sensitivity of parental SiHa to radiation with minimal colony at 4 Gy and very few colony at 8 Gy. Contrarily higher colony forming ability of SiHa/RR cells even after irradiation with acute dose of 4 Gy

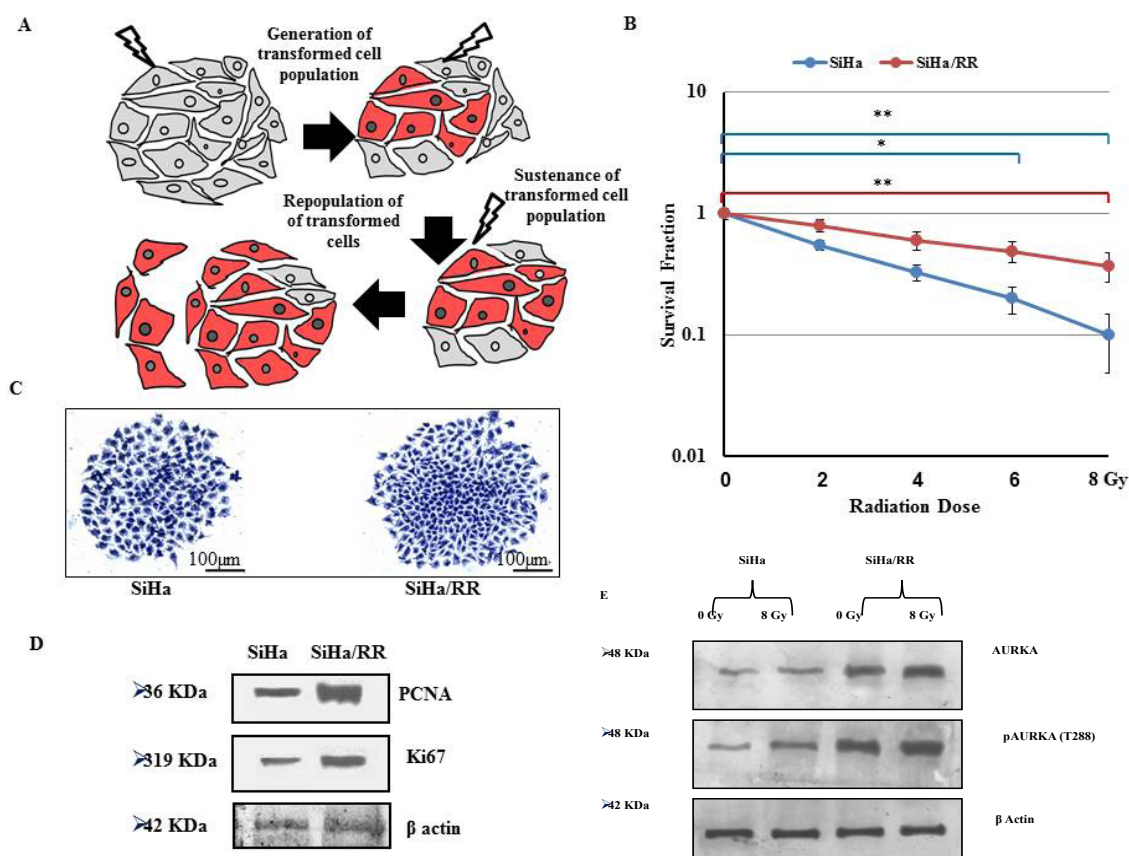


Figure 1. Development and Confirmation of Radioresistance of SiHa/RR: A. Schematic representation showing development of radioresistant cell line. Parental SiHa cells were exposed to weekly fractionated irradiation up to a total cumulative dose of 40 Gy; thereafter isolated and designated as SiHa/RR. B. Survival fraction curves derived from colony formation assay of parental SiHa vs radioresistant SiHa/RR cells exposed to different doses of radiation (0, 2, 4, 6, 8 Gy). The values are mean \pm SD of three independent experiments. * $p < 0.001$, ** $p < 0.0001$. C. Representative images showing average colony size of SiHa and SiHa/RR formed after 3 weeks of cell seeding. Crystal violet stained colonies were observed under inverted microscope (Olympus); at 40X magnification showing the colony of SiHa (left panel) and SiHa/RR (right panel) respectively. D. Expression levels of proliferative markers (PCNA, Ki-67) in SiHa and SiHa/RR cells as observed by western blot analysis using β actin as loading control. E. Expression pattern of Aurora Kinase A (AURKA), pAurora Kinase A (pAURKA T288) in SiHa and SiHa/RR cells as observed by western blotting. β -actin was used to ensure equal protein loading.

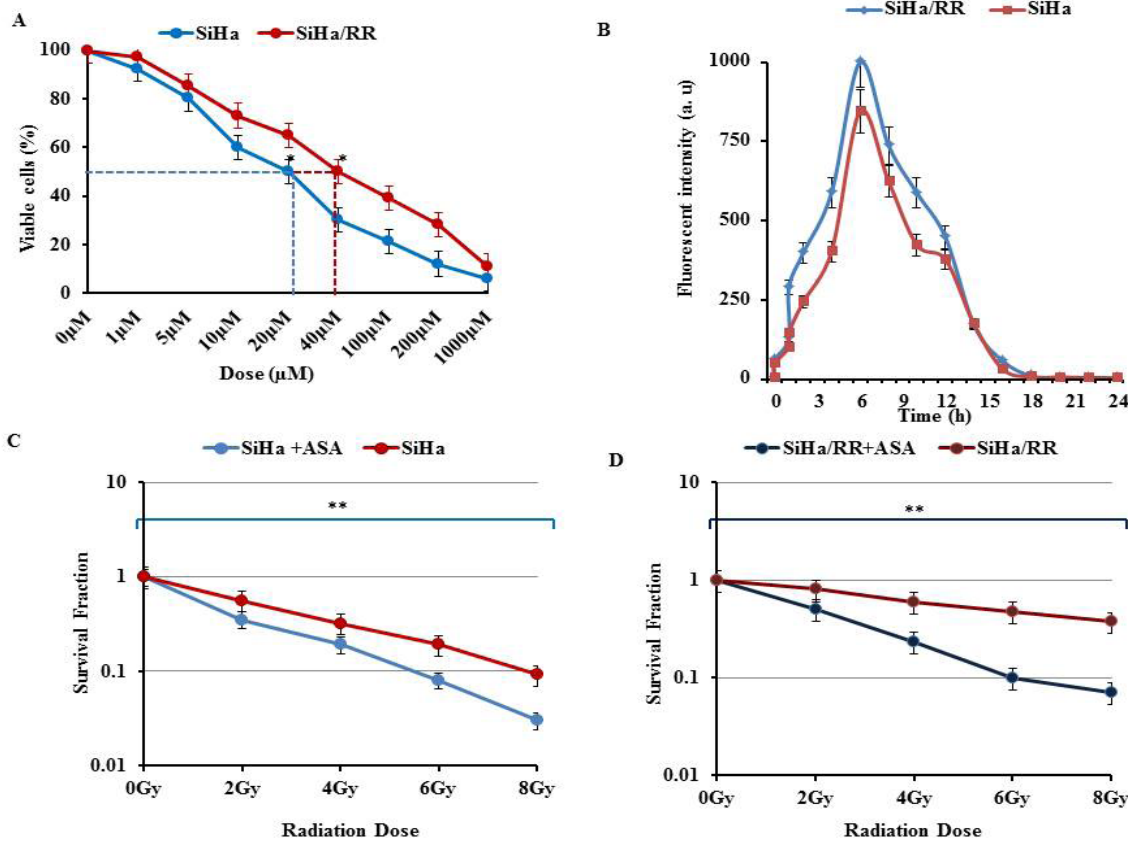


Figure 2. ASA Exerts Improved Radiosensitivity in SiHa/RR: A. Percent viability of SiHa and SiHa/RR cells treated with a wide dose range of ASA for 24 h as measured by MTT assay. Values are expressed as Mean \pm SD of at least three independent experiments performed in triplicate. B. Determining the intracellular ASA uptake by spectrofluorimetric analysis of SiHa and SiHa/RR cells upon exposure to the IC₂₀ dose for different time periods. Analysis was done at an excitation wavelength of 280 nm and emission wavelength of 460 nm. Fluorescence intensities are average values of three independent experiments. The error bars indicate the standard deviation at each wavelength. C. & D. Surviving fractions of SiHa (C) and SiHa/RR (D) calculated from clonogenic assay upon exposure to effective dose of ASA (5 μ M for 6h) followed by challenge with radiation dose of 0, 2, 4, 6, 8 Gy respectively. The values obtained are Mean \pm SD of three independent experiments, * p < 0.001, ** p < 0.0001

indicated significant increase in radioresistance as opposed to parental SiHa. The representative colonies were displayed in Supplementary Figure (S.1). Cell survival was analysed using linear quadratic model. Surviving fractions (number of colonies formed after irradiation/total number of cells seeded \times plating efficiency) were calculated for each dose of radiation, plotted graphically (Figure 1B). The Corresponding D₀ (dose at which the survival is reduced to 37%), D₁ (dose at which the survival is reduced to 90%) and SF₂ (Survival fraction of cells at 2 Gy radiation) were calculated and found to be much higher in SiHa/RR; implying its radioresistant phenotype. The calculated values were tabulated in supplementary file 2 (S.2A). Additionally, differential clonogenic efficiency in SiHa and SiHa/RR cells were evidenced from number of cells per colony, which were much higher in SiHa/RR cells than in SiHa (Figure 1C); signifying the increased proliferative potential of the resistant subline. Elevated expression of proliferative markers (Ki-67 and PCNA) furthermore strengthened the notion (Figure. 1D). Expressions of Aurora Kinase A (a critical regulator of mitotic cell proliferation) was observed by western blotting. Upregulation of Aurora Kinase A and

its activated form pAurora Kinase A in resistant subline gave an indication of mitotic dysregulation succeeding proliferation in SiHa/RR (Figure 1E).

Exposure of SiHa and SiHa/RR cells to ASA gave rise to inhibition of cell proliferation by improving radiosensitivity

To investigate the growth inhibitory effect of ASA, SiHa and SiHa/RR cells were treated with increasing concentration of ASA with concentration range of 1 μ M to 1 mM. MTT assay results depicted significant reduction in cell viability in a dose dependent manner in ASA treated cells in comparison to untreated cells (Figure 2A). Based on MTT results IC₁₀-IC₉₀ values were calculated and were tabulated (S. 2B). An approximate sub-optimal dose of IC₂₀ was selected (5 μ M) for all the subsequent experiments conducted in SiHa and SiHa/RR. It was thereafter felt interested to check the time dependent intracellular accumulation of ASA to ascertain the time at which its maximum accumulation takes place. Considering the auto-fluorescence property of ASA, spectrofluorimetric assay was performed in both treated and untreated SiHa and SiHa/RR cells. The maximum mean fluorescence

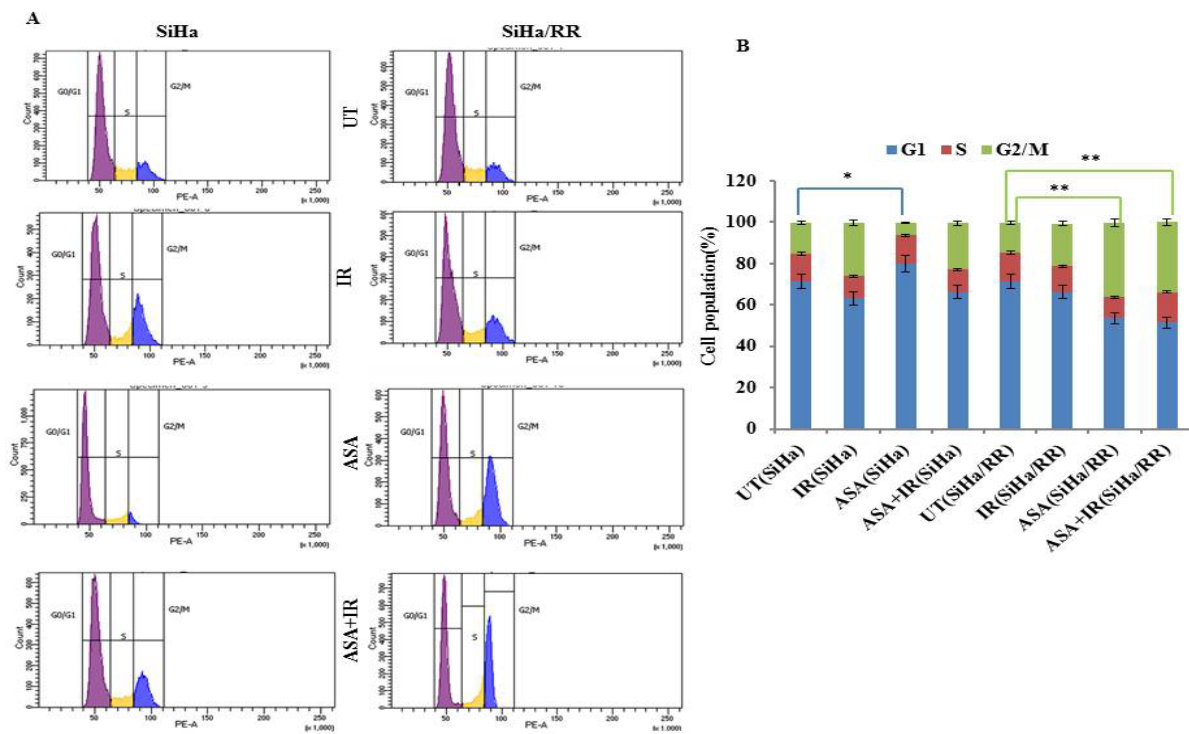


Figure 3. Effect of ASA and/or Radiation on Cell-Cycle. A. SiHa (left panel) and SiHa/RR (right panel) cells were exposed to ASA (5µM) for 6 h; with or without post-exposure to radiation (4 Gy). Distribution of cells at different phases was measured by flow cytometry succeeding PI staining. Untreated cells were taken as control. B. Frequency distribution of cells after quantification of cells at different phases of cell-cycle has been represented graphically. Data (Mean ± SD) are representative of three independent experiments. *p< 0.001, **p< 0.0001 refers deviation from untreated control cells.

intensity of ASA was observed after 6 h of incubation at an absorption maxima of 460 nm (excitation 280; emission 460 nm); specifying its optimum uptake within 6 h. Later on, the graph showed a declining trend due to reduction in

accumulation of ASA (Figure 2B). The curve interestingly showed improved accumulation of ASA in SiHa/RR cells as compared to SiHa.

Based on these findings, optimum treatment condition

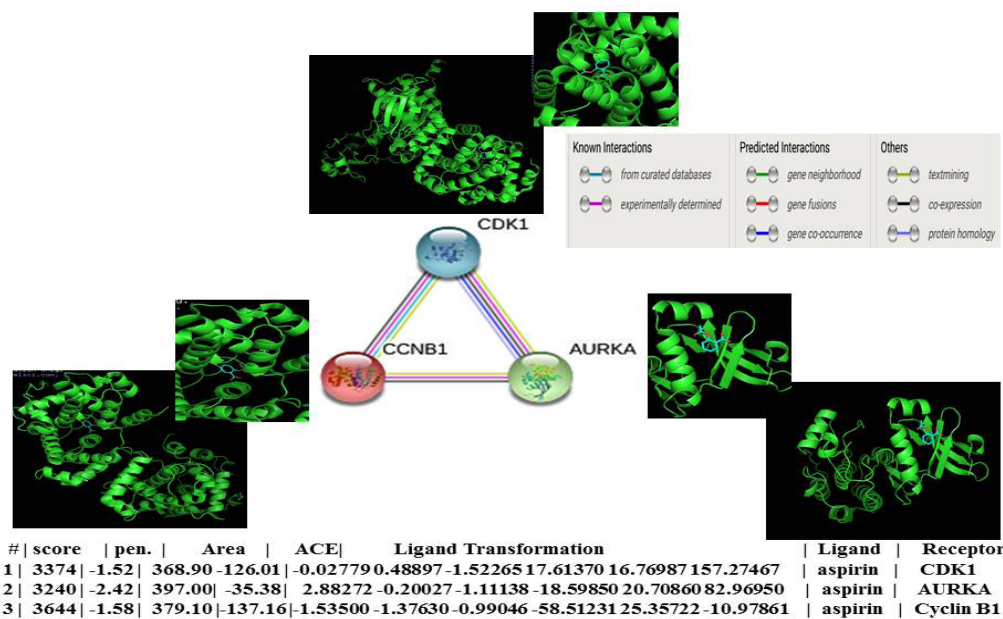


Figure 4. *In Silico* Data of Interaction of ASA with Regulators of G2/M Phase: Interaction between proteins (Aurora Kinase A or AURKA, Cyclin B1 and CDK1) functionally involved in G2/M was assessed by STRING network analysis. Corresponding *In Silico* docking analysis among ASA-CDK1, ASA-Cyclin B1 and ASA- Aurora Kinase A (AURKA) was done in FireDock and were visualized in Pymol software. Representative values are enlisted in tabular form.

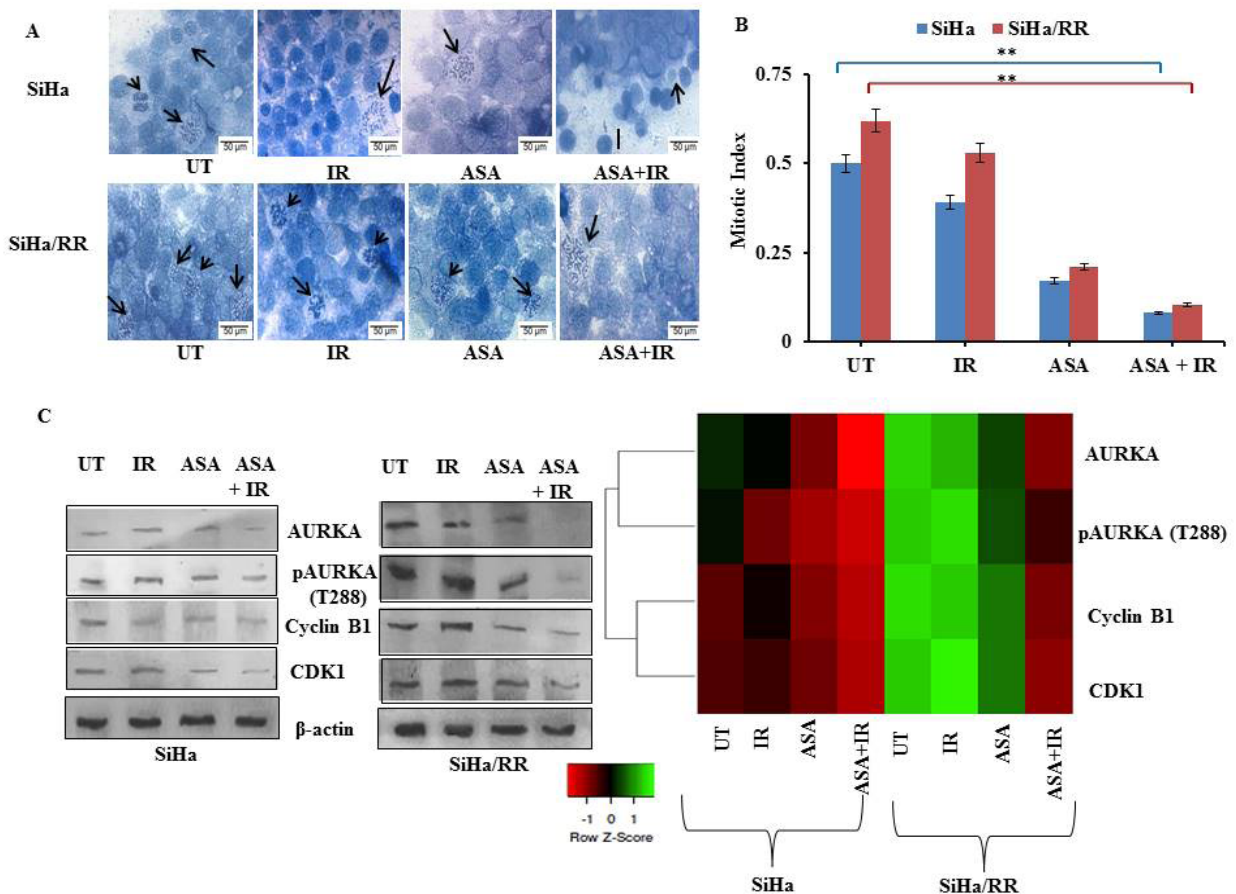


Figure 5. Effect of ASA on Mitosis. A. Morphological observation (Inverted microscope: Olympus) of Giemsa stained SiHa (upper panel) and SiHa/RR (lower panel) cells showing prominent chromosomal alignment in mitotic cells as indicated by black arrows. Original images are 400X, scale bar 50 μ m. B. Mitotic Index as calculated by the ratio of numbers of mitotic cells to total number of cells of SiHa and SiHa/RR was plotted graphically. The values obtained are Mean \pm SD of three independent experiments, $**p < 0.0001$. C. Parental SiHa and resistant SiHa/RR cells were subjected to western blotting to check the expression of Aurora Kinase A (AURKA), pAurora Kinase A (pAURKA T288), Cyclin B1, CDK1 (left panel). Band intensities of each band were calculated by ImageJ Software and represented by heatmap (right panel). Fold change of expression is indicated in color gradient (color toward green indicates higher protein expression levels and color toward red indicates lower expression levels as compared to untreated control)

(dose and time) of ASA for upcoming experimentations were determined. Prior to obtain the absorption maxima, experiment was conducted to measure fluorescence intensity of treated cells at different excitation emission spectra. Maximum fluorescence intensity was obtained at a wavelength of 460 nm which was considered as the absorption maxima (S. 2C).

Clonogenic viability assay was re-performed in the presence and absence of ASA for assessing its potential in restoring radiosensitivity, particularly in SiHa/RR. Microscopic observation depicted enlarged colony with much higher number of cells in SiHa/RR than parental SiHa in untreated condition. ASA treatment reduced average colony size in SiHa/RR cells. Representative images have been provided in supplementary file (S. 3A). Survival curves, based on survival fractions calculated for SiHa (Figure 2C) and SiHa/RR (Figure. 2D) were plotted graphically. The surviving fractions (SF2) in ASA treated cells and more importantly in case of combination of ASA and radiation were appreciably diminished (Figure 2C and D). The corresponding D0, D1, SF2 values were

calculated (S. 3. B). Evidentially, reduced SF2 value from 0.6 ± 0.02 to 0.36 ± 0.06 for SiHa and from 0.71 ± 0.18 to 0.5 ± 0.09 for SiHa/RR; hinted about the radio-sensitizing ability of ASA.

Analysis of cell-cycle progression after exposure of SiHa and SiHa/RR cells to ASA and/or radiation

IR activates the cell-cycle checkpoint in radiosensitive cells to prevent cell division and thus provides requisite time for DNA damage repair. Radioresistant cells however, exhibit faulty cell-cycle check point regulation as an effect of radioadaptive response acquired by them. Therefore, cell-cycle analysis was performed in SiHa/RR cells using BD LSR Fortessa Flowcytometer to identify ASA mediated amelioration of radiosensitivity. Both SiHa and SiHa/RR cells were pre-treated with ASA for 6 h alone or, thereafter subjected to irradiation and afterwards processed with PI staining for analysis. In untreated SiHa and SiHa/RR cells, barely any change in the percentage of cell population at different phases was noticed (Figure 3A). Radiosensitive cells underwent G2/M

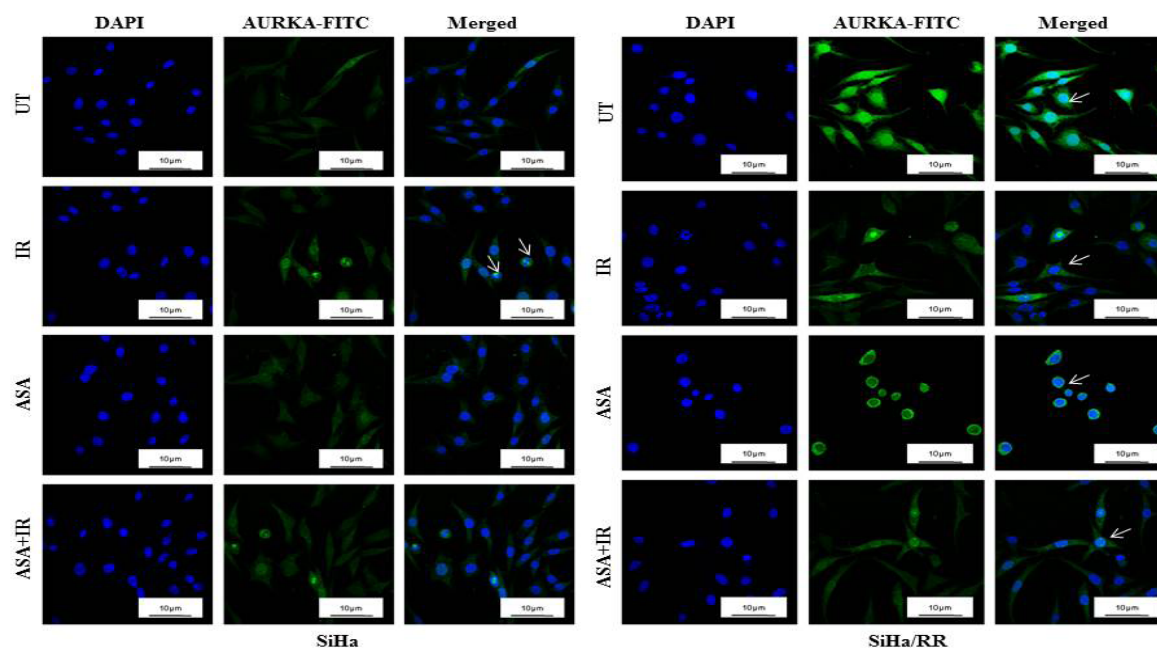


Figure 6. ASA Mediates Radiosensitization by Negatively Regulating Aurora Kinase A: Confocal microscopic images of Aurora Kinase A or AURKA positive (FITC) cells in untreated and treated SiHa (left panel) and SiHa/RR cells (right panel). Cells are showing DAPI stained nucleus. Images were captured under Leica TCS-SP8 microscope and were visualized using LasX software. Original magnification 630X, scale bar 10 μ m. Arrows indicate reduced frequency of Aurora Kinase A expression in treated groups.

arrest upon irradiation, while SiHa/RR efficiently escaped the radiation induced arrest. ASA (6 h) pre-treated SiHa cells experienced marginal increase in population at G₀/G₁ phase whereas remarkable arrest of cells at G₂/M phase was observed for SiHa/RR. Simultaneous decrease of cell population at G₁ phase was noted particularly in SiHa/RR cells (Figure 3A). Furthermore the result exhibited that ASA exerted better effect in inducing arrest in SiHa/RR cells; may be due to better accumulation of ASA in resistant subline. (as depicted in Figure 2B). Graphical representation showing percentage of cell population at different phases also exhibited similar trend for SiHa and SiHa/RR (Figure 3B). The G₂/M population in SiHa/RR cells was increased upto 2.5 fold from 14.4% in untreated to 36.1% in ASA treated cells as well as upto 2.34 fold in combinatorial treatment modality with radiation from 14.4% in untreated to 33.7% in ASA treated cells.

ASA binds efficiently with the G₂/M regulator

The significant arrest of SiHa/RR cell population upon treatment with ASA alone or in ASA+IR groups gave an indication towards ASA mediated regulation of G₂/M proteins. This interesting observation prompted to look into the binding patterns of these proteins with ASA. The interaction between these mitotic regulators was evidenced from String Database analysis. *In silico* molecular docking analysis was performed in FireDock software to explore the possible interaction of ASA with such G₂/M proteins like Aurora Kinase A, Cyclin B1 and CDK1. The visualization of docking result was performed in pymol software. Results displayed convincing binding of ASA at the catalytic domain of Aurora Kinase A

and CDK1 and at the activation site of Cyclin B1. The binding score, ACE and ligand transformation value was satisfactory; highlighting the suitable interaction of ASA with the G₂/M specific proteins (Figure 4).

Mitotic index after irradiation is altered by ASA

To examine whether ASA treated SiHa and SiHa/RR cells altered its mitotic ability, mitotic index was measured. Mitotic cells were observed under an inverted microscope in (UT), (IR), (ASA), (ASA+IR) cells (Figure 5A). Number of mitotic cells was observed based on the pattern of chromosomal alignment. Number of mitotic cells were significantly high in SiHa/RR (lower left panel) compared to SiHa (upper left panel). Radiation exposure reduced the frequency of mitotic cells in SiHa but not in SiHa/RR. Interestingly, ASA treatment invariably restrained the prevalence of mitotic cells in both the cell lines; distinctly in SiHa/RR, when treated in combination with radiation. Mitotic index as calculated by the ratio of number of cells undergoing mitosis to total number of cells was decreased significantly in ASA treated cells; which further reduced in ASA pre-treated irradiated cells; implying impaired mitotic ability in ASA treated cells either alone or even in combination with radiation (Figure 5B). To determine the mechanism of mitotic block induced by ASA, expressions of mitotic (G₂/M) regulators like Aurora Kinase A, pAurora Kinase A (Thr 288), CDK1 and Cyclin B1 were assessed by western blotting. The result (Figure 5C left panel), illustrated substantially increased expressions of Aurora Kinase A and pAurora Kinase A in SiHa/RR cells contrasted to SiHa. Similar trends were observed for specific G₂/M regulatory

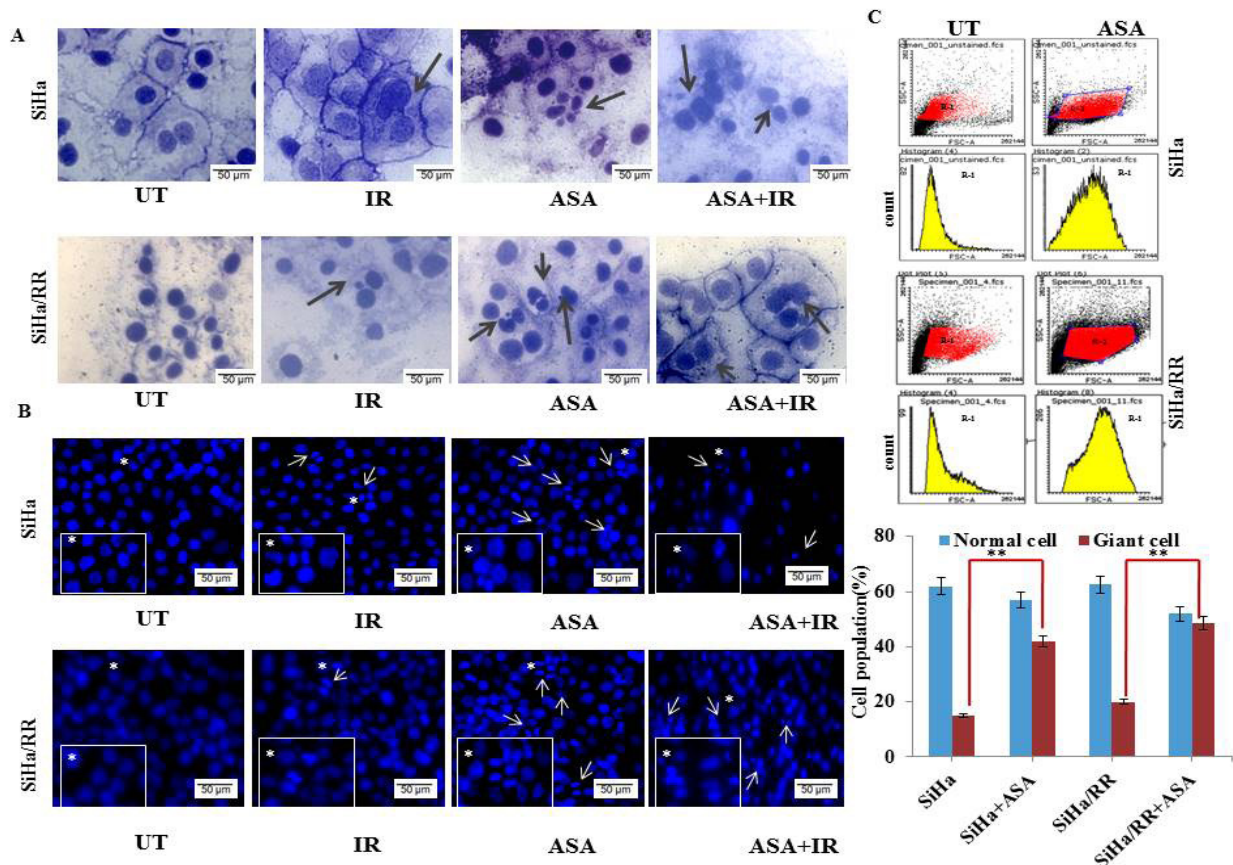


Figure 7. SiHa and SiHa/RR Cells were Compelled to Undergo Mitotic Catastrophe by ASA: A. Both SiHa (upper panel) and SiHa/RR (lower panel) cells were either pre-treated with ASA or radiation dose (4 Gy) or ASA pre-treatment 6 h followed by IR (4 Gy). Cells were stained with Giemsa after 24 h incubation. Morphological observation under inverted microscope (Olympus) revealed increased frequency of giant cells with micronucleation and multinucleation (Black arrows) upon ASA treatment alone or in combination with radiation compared to untreated or only radiation treated cells. Original images are 400X, scale bar 50 μ m. B. DAPI stained cells were examined under fluorescence microscope (Olympus) to check ASA induced nuclear changes. Visible characteristic features (enlarged nuclei, micronucleated, multinucleated cells, cells with distorted spindle and nuclear fragmentation) are shown in white arrows in ASA treated cells in the presence and absence of radiation treatment. Original images are 400X, scale bar 50 μ m. C. Graphical representation of calculated frequency of ASA treated giant cells in SiHa and SiHa/RR cells. Results were obtained from flow cytometric analysis by gating the cells (R-1) in side scatter (Y axis) vs forward scatter (X axis). Experiments were performed in triplicate. The values obtained are Mean \pm SD of three independent experiments, ** $p < 0.0001$.

markers Cyclin B1/CDK1. However, distinguishable inhibitions in expressions of these proteins were noticed upon ASA treatment. ASA exposed irradiated cells appreciably reduced the expressions of these proteins, which furthermore strengthened the notion of restoring radiosensitive ability of SiHa/RR by ASA. Calculation of band intensities by ImageJ Software and subsequent representation by heatmap (right panel) displayed clear corroboration of the findings.

ASA by negatively regulating Aurora Kinase A restores radiosensitivity in SiHa/RR cells

To ascertain whether ASA exerts its radiosensitizing potential in SiHa/RR cells by targeting Aurora Kinase A, immunofluorescence assay was performed. Both SiHa and SiHa/RR cells (untreated or treated) were subjected to immunofluorescence analysis with antibodies against Aurora Kinase A (FITC, green) and to staining with DAPI (blue). Confocal microscopic images (Figure 6) displayed high Aurora Kinase A positive cells (nucleus as well as

cytosol) in untreated SiHa/RR (right panel) unlike SiHa cells (left panel with minimal nuclear Aurora A Kinase). Treatment with ASA in cells with eventual irradiation decreased the frequency of Aurora Kinase A positive cells, specifically in SiHa/RR. These findings substantiated the previous observation of western blot analysis and ASA treated mitotic block was validated by attenuated Aurora Kinase A expression. Images were captured under Leica TCS-SP8 microscope and were visualized using LasX software. Original magnification 630X, scale bar 10 μ m. Arrows indicated reduced frequency of Aurora Kinase A expression in treated groups.

ASA triggers Mitotic Catastrophe in radioresistant cells

Confirmation of ASA mediated mitotic catastrophe as consequence of downregulated Cyclin B1, CDK1 and Aurora Kinase A, was performed by microscopic examination of Giemsa as well as DAPI stained cells. Microscopic observation revealed normal rounded nuclear morphology in untreated cells (Figure 7A). Visible nuclear

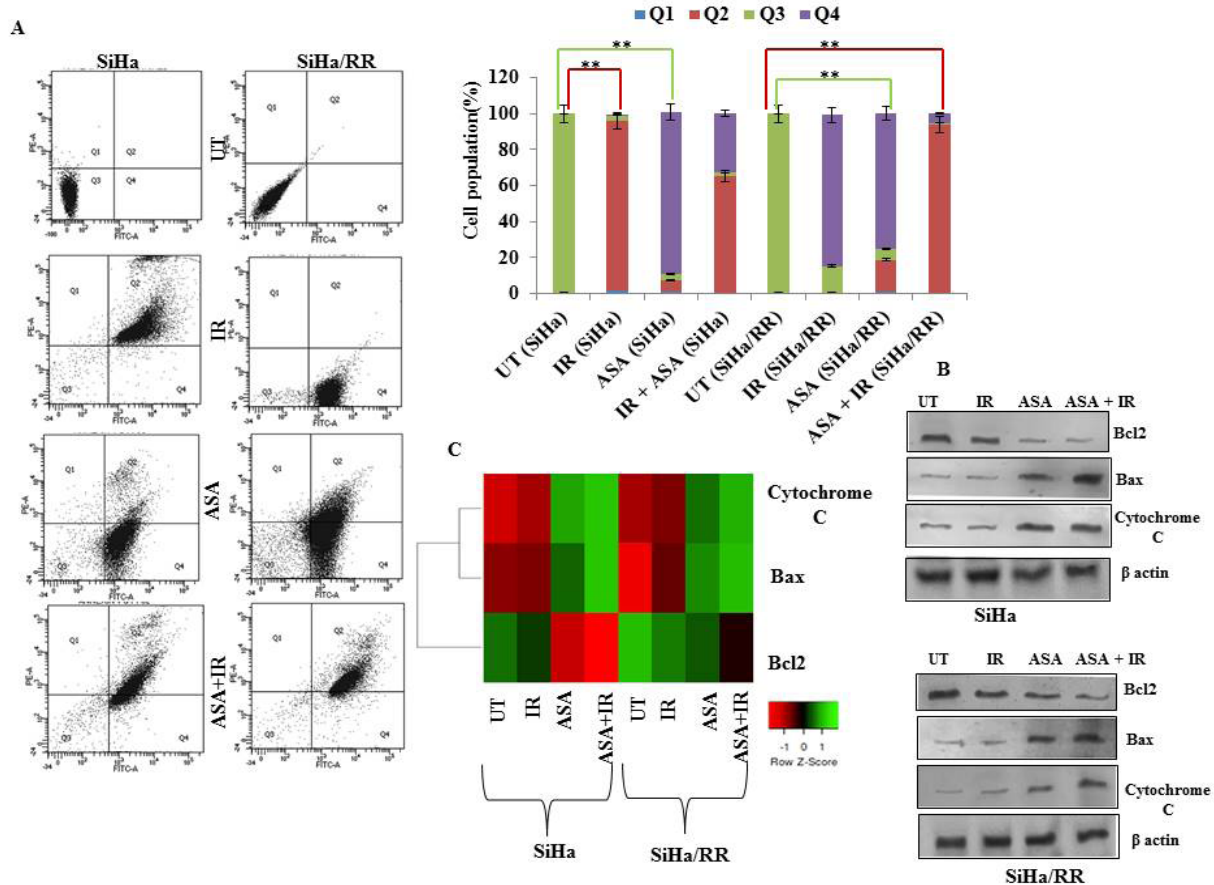


Figure 8. Estimating the Impact of ASA and/or Radiation on Apoptosis: A. Representative flowcytometric charts of AnnexinV-FITC/PI stained SiHa (left panel) and SiHa/RR (right panel) in untreated cells or cells treated with ASA and/or IR. Q1 represents necrotic cells, Q2 late apoptotic cells, Q3 live cells and Q4 early apoptotic cells. Corresponding graphs indicating cell population (percentage) has been represented in Q1, Q2, Q3, Q4 quadrants of SiHa and SiHa/RR. The values obtained are Mean \pm SD of three independent experiments, $**p < 0.0001$. B. Expression of proteins associated with apoptosis (Bcl2, Bax, Cytochrome C) in SiHa and SiHa/RR cells. β -actin was used as loading control. C. Heatmap analysis was performed as described above in details.

damages was evident in SiHa while was insignificant in SiHa/RR when challenged with IR. Incubation of cells with ASA (5 μ M) resulted in condensed pyknotic nuclei, multiple nuclei or higher frequency of micronuclei; indicative of mitotic catastrophe as a consequence of abnormal mitosis. All the possible nuclear alterations caused by ASA (A) asymmetric nuclear division, (B) chromosomal arrest, (C) multiple nuclei with micronuclei, (D) quadri-nucleated cells, (E and F) Giant multinucleated cells denoted typical morphological characteristics of mitotic catastrophe (S. 4). Images were captured at a magnification of 400X, scale bar 50 μ m. DAPI stained cells (Figure 7B), when observed under fluorescent microscope exhibited significant alteration in the nuclear morphology. This alteration was accompanied with much higher frequency of micronuclei with notable uprise in number of cells accompanied by visibly distinct chromosomes upon ASA exposure as well as in combination treatment. Photomicrographic findings were confirmed by flow cytometric analysis for determining the cell size using forward scatter vs side scatter analysis (Figure 7C). This result additionally demonstrated increased frequency of Giant cells upon ASA treatment; particularly in SiHa/RR cells (Figure 7C; lower panel). These flow cytometric

findings thus supported the impression that ASA may act as a stimuli to induce mitotic catastrophe in radioresistant cells.

ASA mediated mitotic catastrophe is followed by apoptosis

Next objective was to ascertain whether the event of mitotic catastrophe serves as a precondition for cells to undergo apoptosis subsequently. To accomplish the objective, SiHa and SiHa/RR cells were pre-treated with ASA (5 μ M) for 12 h instead of 6 h (optimum incubation time for mitotic catastrophe) followed by exposure (with / without) to acute dose of radiation. Irradiation dose was selected as 8 Gy instead of 4 Gy as SiHa/RR showed maximum resistance towards 4 Gy with a marginal sensitivity towards 8 Gy (Figure 1B). Flow cytometric analysis was performed to examine the frequency of Annexin-V/PI stained cells. The result clearly demonstrated predominant distribution of untreated cells in Quadrant 3, which is considered as Annexin V/PI dual negative live cells. Irradiated SiHa/RR were observed in Quadrant 4 (Annexin V positive and PI negative); signifying early apoptotic cells. Contrarily, SiHa cells were distributed in Quadrant 2, which are Annexin V/PI dual positive; denoting cells at late apoptotic stage. However,

upon incubation of both the cells with ASA, majority of SiHa and SiHa/RR cells were in early apoptotic stage (Quadrant 4); although percentage of late apoptotic cells (Quadrant 2) in case of SiHa/RR was much higher compared to parental SiHa. Interestingly, combinatorial treatment significantly augmented the percentage of late apoptotic cells (Quadrant 2) for both resistant and sensitive cells. This result clearly implied the induction of apoptosis by ASA when exposed for an extended period of time. Cell populations (%) in different quadrants were calculated and represented graphically (right panel Figure 8A). The obtained graph also clearly depicts a significant increase of early apoptotic cells 90.5% after ASA exposure in SiHa and 75.5% in SiHa/RR cells. Since perturbation of Bcl2/Bax ratio fosters the release of Cytochrome C from mitochondria, therefore expressions of these proteins were investigated in both SiHa and SiHa/RR cells. The result inferred an increase in expression of Bax vis-à-vis downregulation of Bcl2 with concomitant increase in cytosolic Cytochrome C expression (Figure 8B); further supporting the apoptotic event induced by ASA. Heatmap analysis was performed to corroborate the results obtained from western blotting (Figure 8C).

Discussion

Recurrent failure to radiotherapy due to acquirement of radioresistance is a burning issue and the molecular mechanism underneath this needs addressal. One of the important features of radioresistant cells is the presence of faulty checkpoint regulators that are unable to cause sufficient arrest or induction of cell death. Therefore, strategy could be adapted to induce cell death by non canonical pathways, particularly by restoring radiosensitivity in cancer cells by repurposing conventional drugs. ASA is one such promising agent that by acting as a radiosensitizer potentially improves disease outcome by lowering radiation doses at a much lower costs (Khan et al., 2019; Sun et al., 2018,). The present study attempted to explore the key mechanism of ASA mediated radiosensitization in cervical cancer cells. The developed radioresistant cell line SiHa/RR differed from parental SiHa cell by reduced radiosensitivity and enhanced proliferative efficiency as observed from the gain in the ability of colony formation; denoting increased survival fraction even after exposure to acute doses of radiation. Enhanced proliferative potential was also supported by upregulated expressions of proliferative markers (PCNA and Ki-67) along with functional activation of mitotic protein Aurora Kinase A. To execute the mechanistic study, optimum condition for ASA treatment was first determined by MTT assay and intracellular accumulation study. MTT result evidenced anti proliferative efficacy of ASA in SiHa and SiHa/RR cells. To explore ASA as a radiosensitizer, IC₂₀ (sub-optimal) dose as obtained from MTT result was selected as the ideal treatment condition in the present study. Most exciting observation of this study is the difference in intracellular accumulation of ASA between SiHa and SiHa/RR cells showing much higher fluorescence intensity; indicating greater accumulation in SiHa/RR than SiHa. Clonogenic viability assay showed

the most effective reduction in survival fraction at the combination of 5 μM ASA and 4 Gy IR. Accordingly, this combination was used in subsequent experiments. SiHa/RR cells were found to be protective against the radiation induced G2/M arrest, while ASA treatment attributed significant G2/M arrest. G2/M arrest is considered as a key deciding factor of the cytostatic action of ionizing radiation since such arrest prevents cells from entering the mitotic phase (Nahar et al., 2014; Krueger et al., 2010). Earlier reports suggested ASA mediated increased population of cells in the G0/G1 phase with reduced population at S and G2/M phases (Boueroy et al., 2017); although present study clearly explained obvious G2/M arrest in combinatorial treatment which may be due to exposure to sub-optimal dose. These findings demanded further experimentation to check the expressional status of G2/M regulatory proteins like Aurora Kinase A, Cyclin B1 and CDK1 for understanding the underlying mechanism. The Cyclin B1/CDK1 heterodimer was reported to induce mitosis by subsequent phosphorylation and activation of numerous substrates including microtubule effectors (Liu et al., 2020; Jackman et al., 2020, Singh et al., 2021). Aurora Kinase A, is reported to be activated downstream of Cyclin B1/CDK1; and thus performs proper entry into mitosis by controlling G2 checkpoint. Overexpression of Aurora Kinase accelerates abnormal G2/M transition in mammalian cells; resulting into chromosome instability with eventual development and progression of malignant tumors (de Gooijer et al., 2017; Nikonova et al., 2013). In accordance with these previous reports, *in silico* docking analysis was therefore performed to find out whether ASA could bind with these G2/M regulators. ASA was found to have substantial binding efficiency with Aurora Kinase A, Cyclin B1 and CDK1. Expressional analysis at protein levels by western blotting further envisaged the findings of docking study as the result displayed ASA mediated significant abrogation of expressions of these G2/M regulators. Likewise, decreased frequency of Aurora Kinase A positive cells upon ASA treatment as observed from immunofluorescence study further justified the conviction of previous findings. These findings necessitated to examine the morphological features of SiHa and SiHa/RR cells treated with ASA. Microscopic observation and quantification of Giemsa stained cells exhibited higher prevalence of mitotic cells in SiHa/RR compared to SiHa, which gets diminished in both the cases, particularly in SiHa/RR upon incubation of cells with ASA prior to radiation exposure. This was accompanied by the event of mitotic catastrophe as evident from the formation of giant cells with multinucleation and micronucleation in both SiHa and SiHa/RR. Therefore ASA induced increased frequency of 4n containing cells with distinct morphological features of mitotic catastrophe can be considered as the key findings of this study. Mitotic catastrophe, which occurs during mitosis as a consequence of aberrant mitotic progression, is considered as the fundamental condition or milieu for radiation-induced cell death in cancer which eventually may undergo apoptosis or may remain in the state of permanent cell-cycle arrest (Sia et al., 2020). To understand the exact fate of the cells underwent mitotic catastrophe by ASA, cells were

incubated with ASA for a longer period of time from 6 h to 12 h. Apoptotic parameters were examined in both untreated and treated cells. Annexin V- PI assay revealed that SiHa/RR cells failed to undergo apoptosis upon radiation treatment due to their acquired radioresistant phenotype. SiHa cells conversely responded better to radiation treatment as increased frequency of late apoptotic cells were observed after radiation treatment. Nevertheless, treatment of SiHa/RR cells with ASA prior to radiation exposure significantly increased the population of cells at late apoptotic phase. Additionally increased Bax expression with concomitant decreased Bcl2 expression in ASA treated cells or in combination treatment, confirmed the apoptogenic potential of ASA. Cytosolic release of Cytochrome C due to ASA exposure reconfirmed the transition of catastrophic cells towards apoptosis due to prolonged exposure to ASA. The overall of findings of the study affirmed that ASA restored radiosensitivity of radioresistant SiHa/RR by begetting apoptosis through mitotic catastrophe. Characteristic morphological features of mitotic catastrophe as a result of diminished expression of Aurora Kinase A with Cyclin B1/CDK1 due to ASA exposure of SiHa/RR cells validated this hypothesis of mitotic catastrophe. Previous experimental studies have also reported accelerated incidences of mitotic catastrophe through down regulation of Cyclin B1 and CDK1 (Scaife R 2004). Findings of the present study emphasised preclinical success of ASA in triggering radiosensitization in radioresistant cells through the event of mitotic catastrophe. These observations may encourage administration of this molecule in future, in the factual scenario of radioresistance.

Author Contribution Statement

Salini Das: Primary experimentation, Data collection and analysis and manuscript preparation; Dr. Dilip Kumar Ray: For extending his expert help in the calculation of radiation dosimetry in cell lines; Dr. Debomita Sengupta: Assisted in Data analysis and preparation of the manuscript; Elizabeth Mahapatra: Assisted with Data analysis and literature survey; Souvik Biswas: Performed part of the experimentations and had helped in data analysis; Madhumita Roy: Provided her valuable insights in the interpretation of data and final approval of the manuscript; Sutapa Mukherjee: Designing the project, Planning the experimental set up, assisted with data analysis, interpretation and manuscript checking and final approval of the manuscript.

Acknowledgements

Funding Statement

This research is supported by Council of Scientific and Industrial Research (CSIR), Government of India by providing fellowship and contingency grant. The required infrastructural facilities are provided by DIRECTOR, Chittaranjan National Cancer Institute, Kolkata, INDIA.

Part of Student's Thesis

The study has been approved by the Department of Zoology, University of Calcutta as a part of Ph.D thesis work of Ms. Salini Das.

Ethical Issues

The research work is not based on any human or animal tissue samples. The entire work has been carried out using cell lines as in vitro model system.

Conflicts of interest

The authors declare that they have no conflicts of interests.

References

- Absubhi N, Middleton F, Abdel-Fatah TMA, et al (2016). Chk1 phosphorylated at serine345 is a predictor of early local recurrence and radio-resistance in breast cancer. *Mol Oncol*, **10**, 213–23.
- Bader S, Wilmers J, Pelzer M, Jendrossek V, Rudner J (2021). Activation of anti-oxidant Keap1/Nrf2 pathway modulates efficacy of dihydroartemisinin-based monotherapy and combinatory therapy with ionizing radiation. *Free Radic Biol Med*, **168**, 44–54.
- Bagheri M, Hesari AR, Zia Sarabi P, et al (2018). Antiproliferative effect of aspirin on colorectal cancer cell line. *Iran J Toxicol*, **12**, 1–4.
- Biswas S, Mahapatra E, Ghosh A, et al (2021). Curcumin rescues doxorubicin responsiveness via regulating aurora a signaling network in breast cancer cells. *Asian Pac J Cancer Prev*, **22**, 957–70.
- Boueroy P, Aukkanimart R, Boonmars T et al (2017). Inhibitory effect of aspirin on cholangiocarcinoma cells. *Asian Pac J Cancer Prev*, **18**, 3091–6.
- de Gooijer MC, van den Top A, Bockaj I, et al (2017). The G2 checkpoint—a node-based molecular switch. *FEBS Open Bio*, **7**, 439–55.
- Domogauer JD, de Toledo SM, Howell RW, Azzam EI (2021). Acquired radioresistance in cancer associated fibroblasts is concomitant with enhanced antioxidant potential and DNA repair capacity. *CCS*, **19**, 30.
- El-Benhawy SA, Morsi MI, Fahmy EI, et al (2021). Role of resveratrol as radiosensitizer by targeting cancer stem cells in radioresistant prostate cancer cells (PC-3). *Asian Pac J Cancer Prev*, **22**, 3823–37.
- Galez C, Totis C, Bisio A (2021). Radiation resistance: A matter of transcription factors. *Front Oncol*, **11**, 662840.
- Gong L, Zhang Y, Liu C, Zhang M, Han S (2021). Application of radiosensitizers in cancer radiotherapy. *Int J Nanomedicine*, **16**, 1083–102.
- Hauge S, Mariampillai AE, Rødland GE, et al (2021). Expanding roles of cell-cycle checkpoint inhibitors in radiation oncology. *Int J Radiat Biol*, **2021**, 1–10.
- Huang R-X, Zhou P-K (2020). DNA damage response signaling pathways and targets for radiotherapy sensitization in cancer. *Signal Transduct Target Ther*, **5**, 60.
- Jackman M, Marcozzi C, Barbiero M et al (2020). Cyclin B1-Cdk1 facilitates MAD1 release from the nuclear pore to ensure a robust spindle checkpoint. *J Cell Biol*, **219**, e201907082.
- Jiang W, Yan Y, Chen M, et al (2020). Aspirin enhances the sensitivity of colon cancer cells to cisplatin by abrogating the binding of NF-κB to the COX-2 promoter. *Aging*, **12**, 611–27.
- Khan MK, Nasti T, Buchwald Z, Weichselbaum RR, Kron SJ

- (2019). Repurposing drugs for cancer radiotherapy: Early successes and emerging opportunities. *Cancer J*, **25**, 106–15.
- Krueger SA, Wilson GD, Piasentin E, Joiner MC, Marples B (2010). The effects of G2-phase enrichment and checkpoint abrogation on low-dose hyper-radiosensitivity. *Int J Radiat Oncol Biol Phys*, **77**, 1509–17.
- Lim YC, Roberts TL, Day BW, et al (2012). Therapeutic discovery a role for homologous recombination and abnormal cell-cycle progression in radioresistance of glioma-initiating cells. *Mol Cancer Ther*, **11**, 1863–72.
- Liu JB, Hu L, Yang Z, et al (2019). Aurora-A/NF- κ B signaling is associated with radio-resistance in human lung adenocarcinoma. *Anticancer Res*, **39**, 5991–8.
- Liu K, Zheng M, Lu R et al (2020). The role of CDC25C in cell-cycle regulation and clinical cancer therapy: a systematic review. *J Cell Biol*, **219**, 201907082.
- Barretta ML, Spano D, D'Ambrosio C, et al (2016). Aurora-A recruitment and centrosomal maturation are regulated by a Golgi-activated pool of Src during G2. *Nat Commun*, **7**, 11727.
- Mandati V, del Maestro L, Dingli F, et al (2019). Phosphorylation of merlin by aurora kinase appears necessary for mitotic progression. *JBC*, **294**, 12992–13005.
- Marill J, Mohamed Anesary N, Paris S (2019). DNA damage enhancement by radiotherapy-activated hafnium oxide nanoparticles improves cGAS-STING pathway activation in human colorectal cancer cells. *Radiother Oncol*, **141**, 262–66.
- Marxer M, Ma HT, Man WY, Poon R (2014). p53 deficiency enhances mitotic arrest and slippage induced by pharmacological inhibition of Aurora kinases. *Oncogene*, **33**, 3550–60.
- Mavragani IV, Nikitaki Z, Kalospyros SA, Georgakilas AG (2019). Ionizing radiation and complex DNA damage: From prediction to detection challenges and biological significance. *Cancers*, **11**, 1789.
- Morgan MA, Lawrence TS (2015). Molecular pathways: Overcoming radiation resistance targeting DNA damage response pathways. *Clin Cancer Res*, **21**, 2898–904.
- Nahar K, Goto T, Kaida A, Deguchi S, Miura M (2014). Effects of Chk1 inhibition on the temporal duration of radiation-induced G2 arrest in HeLa cells. *J Radiat Res*, **55**, 1021–7.
- Nikonova AS, Astsaturov I, Serebriiskii IG, Dunbrack RL, Golemis EA (2013). Aurora-A kinase (AURORA A KINASE) in normal and pathological cell growth. *Cell Mol Life Sci*, **70**, 661–87.
- Otani K, Naito Y, Sakaguchi Y, et al (2016). Cell-cycle-controlled radiation therapy was effective for treating a murine malignant melanoma cell line in vitro and in vivo. *Sci Rep*, **6**, 30689.
- Qian J, Zhang Z, Han X, et al (2022). Radiosensitizing effect of celastrol by inhibiting G2/M phase arrest induced by the c-myc gene of human SW1353 chondrosarcoma cells: Network and experimental analyses. *Biomed Res Int*, **2022**, 1948657.
- Sazonova EV, Petrichuk SV, Kopeina GS, Zhivotovsky B (2021). A link between mitotic defects and mitotic catastrophe: detection and cell fate. *Biol Direct*, **16**, 25.
- Scaife R (2004). G2 cell-cycle arrest, down-regulation of cyclin B, and induction of mitotic catastrophe by the flavoprotein inhibitor diphenyleneiodonium. *Mol Cancer Ther*, **3**, 1229–37.
- Schulz A, Meyer F, Dubrovskaya A, Borgmann K (2019). Cancer stem cells and radioresistance: DNA repair and beyond. *Cancers*, **11**, 862.
- Shen Z-T, Chen Y, Huang G-C, et al (2019). Aurora-A confers radioresistance in human hepatocellular carcinoma by activating NF- κ B signaling pathway. *BMC Cancer*, **19**, 1075.
- Sia J, Szymid R, Hau E, Gee HE (2020). Molecular mechanisms of radiation-induced cancer cell death: A primer. *Front Cell Dev Biol*, **8**, 41.
- Singh D, Schmidt N, Müller F, Bange T, Bird AW (2021). Destabilization of long astral microtubules via Cdk1-dependent removal of GTSE1 from their plus ends facilitates prometaphase spindle orientation. *Curr Biol*, **31**, 766–81.
- Sun Y, Dai H, Chen S, et al (2018). Disruption of chromosomal architecture of cox2 locus sensitizes lung cancer cells to radiotherapy. *Mol Ther*, **26**, 2456–65.
- Sung H, Ferlay J, Siegel RL, et al (2021). Global cancer statistics 2020: GLOBOCAN Estimates of Incidence and Mortality Worldwide for 36 Cancers in 185 Countries. *CA Cancer J Clin*, **71**, 209–49.
- Visconti R, Della Monica R, Grieco D (2016). Cell-cycle checkpoint in cancer: a therapeutically targetable double-edged sword. *J Exp Clin Cancer Res*, **35**, 153.
- Woo J. K., Kang J-H, Shin D, et al (2015). Daurinol enhances the efficacy of radiotherapy in lung cancer via suppression of Aurora kinase A/B expression. *Mol Cancer Ther*, **14**, 1693–1704.
- Zhao Y, Moran MS, Yang Q, et al (2012). Metadherin regulates radioresistance in cervical cancer cells. *Oncol Rep*, **27**, 1520–6.



This work is licensed under a Creative Commons Attribution-Non Commercial 4.0 International License.